JOURNAL OF MATERIALS SCIENCE: MATERIALS IN MEDICINE, 6(1995) 297–301

The effects of sintering atmosphere on the chemical compatibility of hydroxyapatite and particulate additives at 1200 °C

A. J. RUYS, A. BRANDWOOD, B. K. MILTHORPE, M. R. DICKSON*, K. A. ZEIGLER‡, C. C. SORRELL‡
Graduate School of Biomedical Engineering, Biomedical Electron Microscope Unit and ‡Department of Ceramic Engineering, University of New South Wales, Sydney, NSW 2052, Australia*

According to Le Chatelier's principle, dehydration and the associated decomposition of hydroxyapatite (HAP) to biodegradable unhydrated calcium phosphates during sintering may be suppressed under a moist sintering atmosphere (thermodynamic effect), or possibly under a pressurized sintering atmosphere (physical effect), by opposing the release of water. The present study explored this possibility. High-purity powdered additives were used to minimize impurity and morphological effects. Al_2O_3, C, SiC, SiO_2, ZrO_2, and 316L stainless steel were all trialled at an addition level of 20 vol%. Heat treatment was at 1200°C for 1 h under two experimental atmospheres and two corresponding control atmospheres: flowing H_2O/O_2 mix—ambient air as a control; pressurized (1 MPa) argon—ambient argon (0.1 MPa) as a control. Specimens were analysed for decomposition by X-ray diffraction (XRD), for densification by porosity measurement, and for microstructural uniformity by energy dispersive spectroscopy (EDS) and image analysis. Significant decomposition occurred under all atmospheres with the exception of flowing H_2O/O_2 which eliminated decomposition in the HAP–Al_2O_3, HAP–ZrO_2, and HAP–316L systems, and reduced the decomposition levels from near completion to ~ 50% in the HAP–SiC and HAP–SiO_2 systems. Moistureless pressurization had little effect. Microstructural uniformity was confirmed. No generalized atmosphere–densification interrelationships were observed.

1. Introduction

Hydroxyapatite [$Ca_{10}(PO_4)_6(OH)_2$] (HAP) is a ceramic material that is chemically similar to bone mineral and consequently is one of the few prosthetic materials characterized as bioactive—capable of undergoing bonding osteogenesis *in vivo*. However, synthetic HAP is characterized by greatly reduced fracture toughness and strength values in relation to cortical bone [1]. This is because synthetic HAP is a fine-grained polycrystalline ceramic while cortical bone is a ceramic–polymer composite material characterized by collagen–fibre–HAP crystallite networks (epitaxy) at the nanostructural level, laminates at the microstructural level, and aligned cylinders (osteons) at the macrostructural level [2]. Therefore, full utilization of the bioactivity of HAP-based bioimplants is dependent on the development of synthetic forms of HAP characterized by high fracture toughness.

Fibre reinforcement is a well known means of improving the fracture toughness of brittle materials. Several authors have studied the effect of fibrous additives on the toughness and strength of HAP. Fibres investigated included stainless steel, titanium Inconel 601, Hastelloy X, Fecralloy, Al_2O_3 [3], $3Al_2O_3.2SiO_2$ [4], SiC [5], and C [6]. HAP–fibre chemical compatibility at sintering temperatures was not investigated in these studies. The literature contains little documentation of the high-temperature compatibility of HAP with fibrous or particulate ceramic or metal reinforcement additives. Documented investigations of the HAP–Al_2O_3, HAP SiO_2, and HAP–C systems have previously been reviewed by the authors [7]. Only non-fibrous additives have been investigated, and in each case, the decomposition temperature of HAP was reduced from the usual range of ~ 1300–1400 °C down to ~ 750–1150 °C in the presence of the additives. The reduction in decomposition temperature varied according to the composition of the additive. Subsequent experimentation by the authors has confirmed these findings [7–9].

The development of fibre-reinforced hydroxyapapite (HAP) presupposes HAP–fibre chemical compatibility at the necessary sintering temperatures. For incompatible mixes, previous findings suggest that the fibrous additive will induce dehydration and subsequent decomposition of the HAP during sintering to unhydrated calcium phosphate phases [7–9]. These phases can include oxyhydroxyapatite,

0957–4530

tetracalcium phosphate, α-tricalcium phosphate and β-tricalcium phosphate (α-TCP and β-TCP) [10]. Their presence is undesirable because these unhydrated calcium phosphates are characterized by enhanced *in vitro* dissolution rates in comparison with pure HAP [10, 11]. Degradation of a fibre–reinforced implant may result in the release of the fibres into the surrounding tissues. However, matrix–fibre reactions may be avoided if a suitable compatible fibre composition or mutually compatible fibre-coating material can be identified and used.

Identification of compatible fibre compositions or compatible coating materials involves identical procedures: high-temperature chemical compatibility trials of homogeneous high-purity HAP-additive test mixtures. Materials suited to coating applications will be characterized by low reactivity with respect to both the HAP and additive phases, and the formation of a bond to the HAP matrix that is amenable to the three-stage crack-bridging toughening mechanism involving the progression, under increasing levels of strain, from elastic bridging to frictional bridging to pullout bridging [12].

The suitability criteria for fibrous reinforcement materials in a HAP matrix are common to all fibre-reinforced ceramic composites: suitable mechanical properties, microstructural consistency, suitable interfacial properties, and chemical compatibility. However, the chemical compatibility consideration is dominant in the case of HAP biomaterials.

Whereas in most matrix–fibre systems, a small or even a high level of interfacial reaction may not adversely affect performance service, in the case of fibre-reinforced HAP, decomposition of the HAP during sintering must be avoided absolutely.

Thus a limit—the decomposition temperature—is imposed on the sintering temperature of reinforced HAP. This has been the case in all 16 HAP–additive systems investigated by the authors using a range of oxide ceramics, nonoxide ceramics, and metals as the additive phase [7–9]. In all cases the decomposition temperature was too low to enable adequate sintering to occur. These findings suggest that the prevention of decomposition during the sintering of HAP–additive samples will probably depend on the development of alternative approaches to sintering. To this end, the present work was based on Le Chatelier's principle which dictates that the presence of H_2O vapour (thermodynamic effect) or a high overpressure (physical effect) should impede the release of water vapour from the HAP and therefore impede decomposition.

These effects have not previously been investigated in HAP-additive systems, with one notable exception: moist atmosphere sintering in the HAP–ZrO_2 system (unstabilized ZrO_2 particulate reinforcement), in which flowing water vapour was found to exert a suppression effect on the ZrO_2-induced HAP decomposition reaction [13].

2. Materials and methods

All additives used were in the form of powders so as to eliminate impurity and morphological effects. The powders used are compiled in Table I. 20 vol% (solids basis) of the additives were mixed with the HAP powder using dry vibro-mixing Spex 8000, (Spex Industries Inc., Edison NJ, 08820, USA), a high-agitation impurity-free mixing process. Ashless perspex mixing media and mill were used to ensure that inorganic impurities would not be added to the samples by abrasion of the mixing mill and media. A 30-min mixing period was used for all samples. The 20 vol% level was chosen since this was within the range for optimal particle packing by gap-grading [14], and therefore corresponded to typical additive levels for fibre-reinforced ceramics.

TABLE I. The raw materials used

Material	Purity (%)	Supplier
Al_2O_3	99.99	Sumitomo Aluminium Ltd, Tokyo, Japan
C	99.5	Cerac Inc., Milwaukee, USA
HAP	98.8	Plasma Biotal Ltd, Tideswell, UK
SiC	99.9	South Coast Refractories Ltd, Bulli, Australia
SiO_2	99.9	Cerac Inc., Milwaukee, USA
ZrO_2	99.0	Cerac Inc., Milwaukee, USA
316L Stnls. Steel	> 99	Sintec Australia Ltd, Melbourne, Australia

The mixtures were pelletized at 80 MPa in a 12.75 mm tool-steel die using stearic acid as a die lubricant, attaining a theoretical density of approximately 50% for all samples during pressing. All pellets were sintered at 1200°C for 1 h since this cycle was found to produce sintering to the closed porosity level (~ 98% dense) while consistently producing 100% HAP yields for additive-free HAP pellets.

2.1. Sintering atmospheres

Investigation of the two potential decomposition-suppression mechanisms–the thermodynamic effect and the physical effect—involved heat treatment of identical sets of HAP-additive mixtures under two experimental atmospheres and two corresponding control atmospheres.

2.1.1. Thermodynamic effect

(i) Experimental: flowing H_2O vapour (~ 150 L/h) entrained in an O_2 feed gas. Purpose-built mullite tube-furnace

(ii) Control: static ambient air Molybdenum disilicide furnace (Ceramic Engineering Furnace Manufacturers, Sydney, Australia)

2.1.2. Physical effect

(i) Experimental: static pressurized (1 MPa) 99.99% pure Ar. Graphite furnace (Model 1000-3560-FP20, Thermal Tech. Inc., California, USA)

(ii) Control: static ambient (0.1 MPa) 99.99% pure Ar Graphite furnace (Model 1000-3560-FP20, Thermal Tech. Inc., California, USA)

2.2. Sample characterization

After sintering, the pellets were analysed for microstructural uniformity, %HAP yield, and densification level, using the following analytical techniques.

2.2.1. Microstructural uniformity

The degree of dispersion of the additive phase throughout the HAP phase was determined by energy dispersive spectroscopy (EDS) measurements (Kevex delta plus EDS analyser, Kevex Instruments, Stanford CA, USA) using a scanning electron microscope (SEM) (Leica Cambridge Stereoscan S360, Cambridge, UK). The EDS data were processed using a microcomputer-based image analysis system (QUANTEX image analysis software, Kevex Instruments, Stanford CA, USA) to determine the particle distribution.

2.2.2. %HAP Yield

This was measured by X-ray powder diffraction (Type PW 1140/00 Powder Diffractometer; N. V. Phillips, Eindhoven, Netherlands) using peak area ratios for the major HAP peak (2.817_{100} hkl = 121) and β-TCP peak (2.880_{100} hkl = 217). β-TCP was the predominant dehydrated calcium phosphate phase detected (traces of α-TCP did appear at high β-TCP levels). The relative error in the peak area ratios was determined by 95% confidence intervals on 10 repeat scans. Using the 95% confidence interval, a given %HAP yield varied no more than ± 1%, both in the case of crushing and remixing the powder sample between X-ray scans, and in the case of rescanning the undisturbed powder sample.

2.2.3. Densification

The degree of densification was determined by measurement of the apparent porosity of the sintered samples. This was determined using hydrostatic weighing in water after vacuum deairing. The relative error in this method was derived from repeated weighings and was found to be in the order of ± 3%.

3. Experimental results

3.1. Microstructural uniformity

Image analyses of the EDS data were compiled in the form of 95% confidence intervals about the 20 vol % distribution level. The deviation from 20 vol % was no greater than ± 1.5% in all cases. The one exception was the HAP–Al_2O_3 system. These samples could not be analysed by EDS because the Al_2O_3 particles were submicron and therefore below the reliable detection threshold of the EDS analysis system. These data suggest that the vibro-mixing procedure produced suitably homogeneous composites. Thus, the decomposition and densification trends found in this study adequately reflect the behaviour of theoretical 20 vol % additive levels in HAP.

3.2. Decomposition

As expected, heat treatment at 1200 °C for 1 h caused no decomposition in the pure HAP samples regardless of sintering atmosphere, since the decomposition temperature of pure HAP is generally found to be above 1300 °C. However, decomposition occurred in all of the HAP–additive systems under the control atmospheres. The effects of the moist and pressurized atmospheres were as follows.

3.2.1. Moist atmosphere

The %HAP yield data for the moist atmosphere and the dry control atmosphere are compiled in the histogram of Fig. 1. The data reveal that the moist atmosphere significantly suppressed decomposition in all of the HAP–additive systems with the exclusion of the HAP–C system in which no experimentation was possible due to rapid oxidation of the additive.

Suppression was complete in three of the systems—HAP–Al_2O_3, HAP–ZrO_2, and HAP–316L stainless steel. As expected, observations of samples from the HAP–316L stainless steel system revealed that suppression came only at the expense of heavy oxidation of the additive. Suppression in the HAP–SiC and HAP–SiO_2 systems, though significant, was only partial. This can probably be explained in terms of the relatively high reactivity in these systems, as evidenced by the relatively low decomposition temperatures reported in these systems in comparison with the HAP–Al_2O_3, HAP–ZrO_2, and HAP–316L stainless steel systems [7].

Thus Le Chatelier's principle was obeyed with respect to the presence of H_2O in the sintering atmosphere.

3.2.2. Pressurized atmosphere

The %HAP yield data for the pressurized atmosphere and the non-pressurized control atmosphere are compiled in the histogram of Fig. 2. These data reveal that pressurization (physical effect) did not suppress the

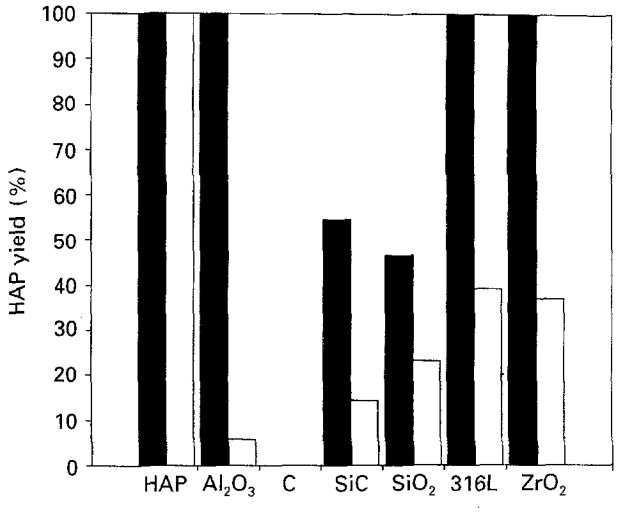

Figure 1 Moist atmosphere effect: %HAP yields after heat treatment at 1200 °C for 1 h. Moist atmosphere (left bar) versus ambient air control atmosphere (right bar).

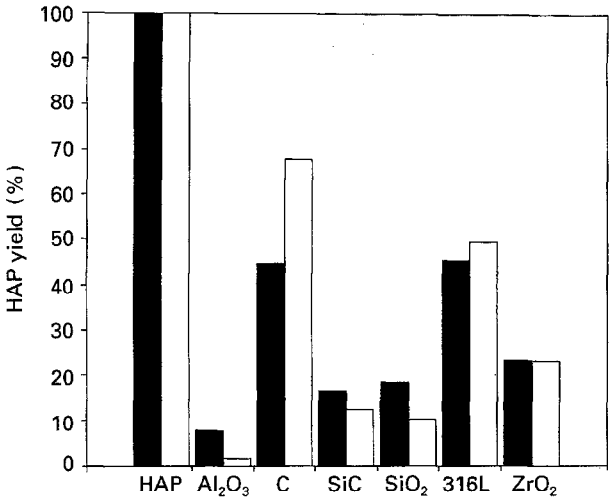

Figure 2 Pressurization effect: %HAP yields after heat treatment at 1200 °C for 1 h. Pressurized inert (argon 1 MPa) (left bar) versus non-pressurized control (argon 100 kPa) (right bar).

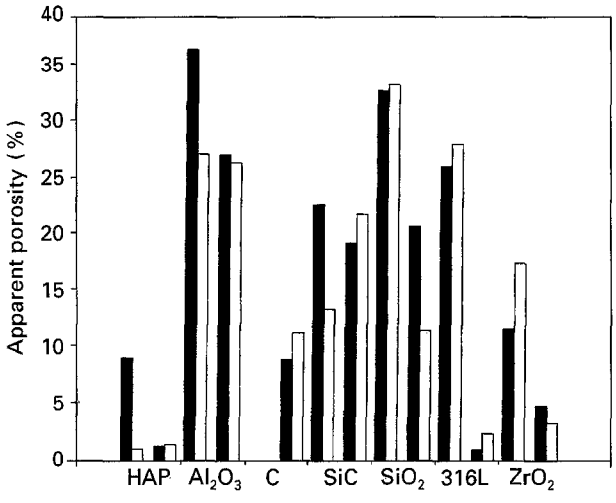

Figure 3 Porosity after heat treatment at 1200 °C for 1 h. The four bars correspond to (left to right): moist atmosphere; ambient air control atmosphere; pressurized inert (argon 1 MPa); non-pressurized control (argon 100 kPa).
Note: Carbon rapidly burned out of the HAP–C composites and so the data for "C" under H_2O/O_2 and air, effectively relate to pure HAP not HAP–C.

decomposition reaction to any noticeable extent in any of the HAP–additive systems, and in the HAP–C system, there was actually a noticeable decomposition enhancement effect. Thus, within the pressure range 100–1000 kPa, pressurization was ineffective as a decomposition-suppression strategy.

3.3. Densification

The porosity data for each of the four sintering atmospheres are compiled in the histogram of Fig. 3. These data reveal that each HAP–additive–atmosphere combination produced a different effect on sintering efficiency. The lack of any clear trends suggests that a complex interaction occurs in each HAP–additive–atmosphere system causing as yet undetermined effects on the coherence of the microstructure.

4. Discussion

The purpose of the present work was the development of sintering protocols that would enable combination of adequate sintering with the elimination of decomposition in these decomposition-prone systems. To this end, the densification data in combination with the decomposition data provided an indication of suitable sintering conditions in each HAP–additive system. Combination of these data suggested the following optimal conditions for each system:

(i) Pure HAP: no decomposition under any atmosphere but sintering was suppressed under the moist atmosphere. Thus dry atmosphere sintering was the preferred option.

(ii) HAP–Al_2O_3: the moist-atmosphere completely suppressed decomposition, although unfortunately this benefit came at the expense of sintering efficiency, which was noticeably reduced in comparison with the dry atmospheres.

(iii) HAP–C: The low oxidation resistance of these samples restricted them to sintering under argon only. Sintered porosites were similar for ambient and pressurized argon, and decomposition was significant especially under pressurization. Thus both options—pressurized inert atmosphere or moist-atmosphere sintering—were detrimental to this system.

(iv) HAP–SiC: The moist atmosphere partially suppressed decomposition although sintering was best under an ambient air atmosphere. Lower temperature moist atmosphere sintering is the best option in this system, although the result will be far from optimal since the porosity was above ~ 20% at 1200 °C.

(v) HAP–SiO_2: The moist atmosphere partially suppressed decomposition, but unfortunately this occurred with an associated porosity of over 30%. Sintering was much better under non-pressurized argon, but with severe associated decomposition. Thus neither option—pressurized inert atmosphere or moist-atmosphere sintering—was suitable in this system, although it is notable that the moist atmosphere did hinder decomposition.

(vi) HAP–316L stainless steel: Decomposition was completely suppressed by the moist atmosphere, but the corrosive effects of the water vapour resulted in poor sintering. Sintering was very efficient under the inert atmospheres but with high associated decomposition levels. Thus neither option—pressurized inert atmosphere or moist-atmosphere sintering—was suitable in this system.

(vii) HAP–ZrO_2: Sintering was completely suppressed under the moist atmosphere and porosity levels were low in all samples, though noticeably lower under the inert atmospheres. Thus a moist atmosphere eliminated decomposition with a small trade-off in sintering efficiency. Therefore, the best overall result occurred in this system.

Acknowledgements

The authors gratefully acknowledge the assistance of Mr C. Martinic and Mr P. Marks, UNSW Biomedical EM unit, with the EDS and image analyses.

References

1. A. J. RUYS, M. WEI, A. BRANDWOOD, B. K. MILTHORPE and C. C. SORRELL, in "Ceramics: adding the value", Vol. 1 (Austceram 92. Proceedings of the International Ceramics Conference. Australia 1992) edited by M. J. Bannister (CSIRO, Melbourne, 1992) p. 586.
2. J. L. KATZ, in "The mechanical properties of biological materials" (Symposia of the Society for Experimental Biology Number 34. Leeds University, 1979) edited by J. F. V. Vincent and J. D. Currey (Cambridge University Press, Cambridge, 1980) p. 137.
3. G. DE WITH and °A. J. CORBIJN, *J. Mater. Sci.* **24** (1989) 3411.
4. S. IIDA, Japanese Patent 62019172, January (1987).
5. A. ENOMOTO, K. MATSUNO, and M. YOKOI, Japanese Patents 01224276, September (1989); 02044074, February (1990); 02051475, February (1990).
6. S. HATAHIRA, European Patent 104640, April (1984).
7. A. J. RUYS, K. A. ZEIGLER, B. K. MILTHORPE and C. C. SORRELL, in "Ceramics: adding the value", Vol. 1 (Austceram 92. Proceedings of the International Ceramics Conference. Australia 1992) edited by M. J. Bannister (CSIRO, Melbourne, 1992), p. 591.
8. A. J. RUYS, N. EHSANI, B. K. MILTHORPE and C. C. SORRELL, *J. Aust. Ceram. Soc.* **29** (1993) 49.
9. A. J. RUYS, B. K. MILTHORPE and C. C. SORRELL, *Interceram.* **43** (1994) 23.
10. L. L. HENCH, *J. Amer. Ceram. Soc.* **74** (1991) 1487.
11. S. R. RADIN and P. DUCHEYNE, *J. Mater. Sci. Mater. Med.* **3** (1992) 33.
12. C. H. HSUEH, in "Composite material technology 1990" (Proceedings of the 13th Annual Energy-Sources Technology Conference and Exhibition. New Orleans, Louisiana, 1990) edited by D. Hui and T. J. Kozik (ASME, New York, 1990) p. 119.
13. K. YAMASHITA, T. KOBAYASHI, M. KITAMURA, T. UMEGAKI and T. KANAZAWA, *Nippon Seramikkusu Kyokai Gakujutsu Ronbunshi* **96** (1988) 616.
14. T. L. STARR, *Amer. Ceram. Soc. Bull.* **65** (1986) 1293.

Received 3 February
and accepted 6 May 1994